



Lightsoft
美国光软

旗舰光学软件

最新2018中文版



GratingMaster® 一维/二维严格光栅设计



DOEMaster® 大角度衍射器件设计

www.lightsoftllc.com

550 MHz carbon nanotube mode-locked femtosecond Cr:YAG laser

Jun Wan Kim (金俊完)¹, Sun Young Choi (崔善英)², Won Tae Kim (金源泰)²,
Bong Joo Kang (姜奉周)², Won Bae Cho (趙元培)³, Guang-Hoon Kim (金光勳)¹,
and Fabian Rotermund (李相旻)^{2,*}

¹Advanced Medical Device Research Division, Korea Electrotechnology Research Institute (KERI), Ansan 15588, Korea

²Department of Physics, Korea Advanced Institute of Science and Technology (KAIST), Daejeon 34141, Korea

³BioMed Research Section, Electronics and Telecommunications Research Institute (ETRI), Daejeon 34129, Korea

*Corresponding author: rotermund@kaist.ac.kr

Received February 9, 2018; accepted April 19, 2018; posted online May 28, 2018

We demonstrate a femtosecond Cr:YAG laser mode-locked by a carbon nanotube saturable absorber mirror (CNT-SAM) at a repetition rate of 550 MHz. By employing the CNT-SAM, which exhibits a modulation depth of 0.51% and a saturation fluence of 28 $\mu\text{J}/\text{cm}^2$ at 1.5 μm , we achieved a compact bulk Cr:YAG laser with self-starting mode-locked operation near 1.5 μm , delivering an average output power of up to 147 mW and a pulse duration of 110 fs. To our knowledge, this system provides the highest repetition rate among reported CNT-SAM mode-locked Cr:YAG lasers and the shortest pulse duration among saturable absorber mode-locked Cr:YAG lasers with repetition rates above 500 MHz.

OCIS codes: 140.4050, 140.5680, 140.7090, 160.4236.

doi: 10.3788/COL201816.061404.

Femtosecond coherent sources with high repetition rates operating near 1.5 μm have been widely investigated for applications in optical communications, optical clocks, analogue-to-digital conversion, electro-optical sampling, and high signal-to-noise ratio nonlinear spectroscopy^[1–5]. Mode-locked fiber lasers can operate stably near 1.5 μm in a compact cavity configuration^[6,7], but it is quite difficult to achieve a high average output power above 100 mW, a pulse duration as short as ~ 100 fs, and a high repetition rate above 500 MHz all at the same time because of the long cavity length and large nonlinearity of the optical fiber. The Cr:YAG laser crystal, one of the representative solid-state laser crystals emitting near the 1.5 μm wavelength, is able to simultaneously provide a high average output power and a high repetition rate with short pulse duration because of its broad gain bandwidth, near 1.5 μm ^[8,9]. To date, most demonstrations have been based on Kerr-lens mode locking, because the small gain and low thermal conductivity of the Cr:YAG crystal make the laser cavity susceptible to intracavity loss^[10–13]. There has only been one report of a high-repetition-rate saturable absorber mode-locked Cr:YAG laser that adopted a saturable Bragg reflector; it exhibited a relatively long pulse duration of about 200 fs^[14].

Carbon nanotube saturable absorbers (CNT-SAs) have been widely employed in a variety of bulk solid-state lasers operating in the 0.8–2.1 μm spectral range because of their broadband nonlinear optical characteristics, including low saturation fluence, controllable modulation depth, and ultrafast recovery time^[15,16]. For high-repetition-rate lasers, the precision of these SA parameters is more important because of the relatively low intracavity peak intensity due to the short cavity length. Near the 1 μm wavelength

range, CNT-SAs with small modulation depths and negligible nonsaturable losses turned out to be applicable for high-repetition-rate mode-locked bulk solid-state lasers^[17,18]. Near the 1.5 μm wavelength range, a CNT-SA that is inserted into the second intracavity of a Cr:YAG laser also provides stable and self-mode-locked operation at a repetition rate of 85 MHz and a pulse duration below 100 fs^[19,20]. However, a CNT-SA mode-locked Cr:YAG laser in a compact scheme with a high repetition rate of above 500 MHz has not been reported until now.

In this work, we demonstrate a CNT-SA mirror (CNT-SAM) mode-locked femtosecond Cr:YAG laser above 500 MHz for the first time. By employing a CNT-SAM, the stable and self-starting mode-locked laser delivers a maximum output power of 147 mW and a 110 fs pulse duration at 550 MHz. To our knowledge, this is the highest repetition rate among CNT-SAM mode-locked Cr:YAG lasers and the shortest pulse duration among saturable absorber mode-locked Cr:YAG lasers with a repetition rate above 500 MHz.

The fabrication process of the CNT-SAM is similar to the one described in Ref. [15]. We used commercially available single-walled CNTs grown by employing the high-pressure carbon monoxide (HiPCO) method. The CNT bundles distributed in the absorber layer show a broadband E_{11} electronic transition located around 1.5 μm . As the first step, the CNTs were dissolved in 1,2-dichlorobenzene (DCB) with a concentration of 0.1 mg/mL and centrifuged. The well-dispersed CNT solution was then mixed with polymethyl methacrylate (PMMA) at a volume ratio of 1:1. Finally, the CNT/PMMA mixture was directly spin-coated onto a high-reflection plane dielectric mirror. At the end of the fabrication process the prepared CNT-SAM was dried

on a hot plate and subsequently in a vacuum oven. The thickness of the SA layer, measured by alpha-step method, was about 200 nm.

To certify the nonlinear optical characteristics of the fabricated CNT-SAM, its nonlinear reflection was investigated using a synchronously pumped near-infrared optical parametric oscillator, delivering 150 fs pulse duration with an output power of 50 mW at 1.5 μm .

From the nonlinear reflection measurement, shown in Fig. 1, we extracted a modulation depth (ΔR) of 0.51%, linear reflection (R_{lin}) of 98.87%, and nonsaturable loss (R_{ns}) of 0.62%, with a saturation fluence (F_{sat}) of 28 $\mu\text{J}/\text{cm}^2$, respectively. The low modulation depth of about 0.5% plays a crucial role in solid-state lasers to suppress undesired Q -switched mode locking and instabilities^[21,22]. The saturation fluence, corresponding to a peak intensity of 0.68 MW/cm^2 , is sufficiently low compared to the intracavity peak intensity, corresponding to the mode-locked threshold.

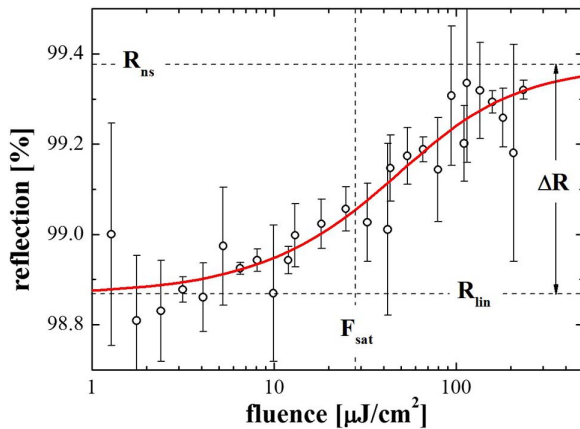


Fig. 1. Nonlinear reflection measurement of the CNT-SAM at 1.5 μm .

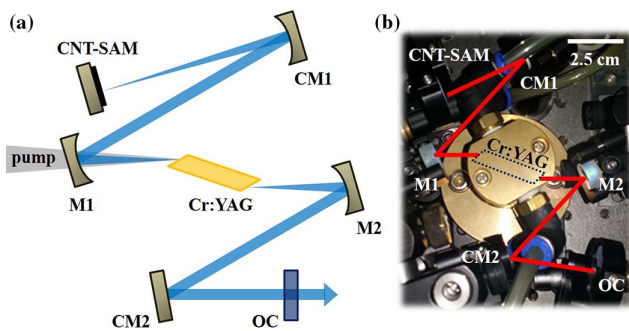


Fig. 2. (a) Schematic and (b) photograph of 550-MHz femtosecond Cr:YAG laser. Cr:YAG: 20-mm-long Cr:YAG gain crystal; M1, M2: HR-coated concave mirrors with $\text{ROC} = -50$ mm; CM1: HR-coated concave GTI mirror with $\text{ROC} = -100$ mm and with one bounce dispersion of -225 fs^2 ; CM2: HR-coated plane GTI mirror with one bounce dispersion of -375 fs^2 ; CNT-SAM: carbon nanotube saturable absorber mirror; OC: output coupler with 0.5% or 0.8% transmission.

Schematic and photographic images of the Cr:YAG laser are shown in Fig. 2. For the short cavity length for a compact laser configuration, a z -folded cavity configuration compensating astigmatism was adopted.

The laser was pumped by a 10 W continuous-wave (cw) single-mode Yb fiber laser (IPG Photonics, YLF-10-LP) operating at 1.064 μm . A 20-mm-long Brewster-cut rod-type Cr:YAG crystal with a diameter of 6 mm was used as the gain medium (MolTech GmbH). Its absorption coefficient was $\alpha = 1$ cm^{-1} at 1.064 μm and a small single-pass absorption was expected, because more than 30% of the incident pump power was transmitted through the Cr:YAG crystal in the range of pump powers above 5.0 W.

The crystal was mounted in a water-cooled copper block whose temperature was maintained at 12°C. It was positioned between two concave mirrors with a radius of curvature (ROC) of -50 mm, M1 and M2, respectively. In the present study, the calculated waist of the cavity mode at the crystal center was 52.7 μm , which is slightly larger than the focused pump beam waist of 44.7 μm . Such relatively large beam waists at the crystal center were used because of the low thermal conductivity of the Cr:YAG crystal.

By enlarging both the pump and cavity mode size at the crystal center, we optimized the output power and the thermal condition of the Cr:YAG laser. For the compact cavity configuration and dispersion compensation, a chirp concave mirror of CM1 and a plane chirp mirror of CM2 were used as folding mirrors. The group delay dispersion (GDD) per bounce of each mirror was -225 fs^2 of CM1 and -375 fs^2 of CM2 at 1.5 μm , respectively. Considering a Cr:YAG crystal GDD of 522 fs^2 at 1.5 μm , the total net cavity dispersion was negative and slightly below -678 fs^2 , which led to a stable and self-starting mode-locking. In the arm side of CM1, CNT-SAM was positioned as the end mirror where the beam waist was estimated to be 92.3 μm . On the other side of the cavity, output couplers (OCs) with 0.8% and 0.5% transmission at the lasing wavelength were used.

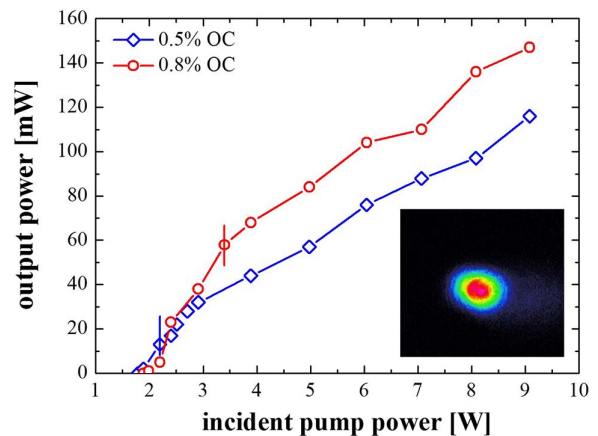


Fig. 3. Average output power versus incident pump power in the femtosecond mode-locked regime, and beam profile of second harmonic generation of mode-locked pulses (inset).

The mode-locked output power generated with the CNT-SAM is depicted in Fig. 3. For the 0.5% OC, the mode-locked threshold was measured to be 13 mW at 3.1 W pumping and the maximum output power was 116 mW at a pump power of 9.1 W. By replacing the OC by 0.8% transmission, the mode-locked threshold was 58 mW at 3.4 W pumping and the maximum output power was 147 mW at a pump power of 9.1 W. In the overall pumping range of the above mode-locked threshold, self-starting mode-locked operation was achieved without spectral modulation or cw spectral components. The intracavity peak intensities corresponding to the mode-locked thresholds were 2.8 MW/cm² for 0.5% OC and 7.9 MW/cm² for 0.8% OC, respectively. These values are much higher than the 0.68 MW/cm² corresponding to the saturation intensity of CNT-SAM. The inset of Fig. 3 shows the far-field beam profile of the mode-locked pulse. Because of the wavelength range limit of the beam profiler (Coherent LaserCam HR), we measured the beam profile of the second harmonic generation of the mode-locked pulse and it clearly exhibited a well-defined single spatial mode.

Figure 4 shows the measured autocorrelation trace and the corresponding spectrum. The intensity autocorrelation function of the pulse was fitted well by assuming a sech² pulse shape and extracting a pulse duration of 110.4 fs. The simultaneously measured spectral bandwidth of 22.6 nm at the center wavelength of 1507 nm leads to a time-bandwidth product of 0.330, which is close to the Fourier transform-limited value of 0.315.

The recorded radio-frequency (RF) spectrum of the laser output is shown in Fig. 5. A pointed peak at the fundamental beat note of 550.0 MHz was measured with a resolution bandwidth of 0.1 kHz within a 400 kHz span. The spectrum shows a high extinction ratio of 67.4 dBc from the background noise level. The inset of Fig. 5 shows the harmonics of the fundamental beat note from the 7.5 GHz wide span measurement of the RF signal. The measured RF spectra clearly indicate a stable single-pulse

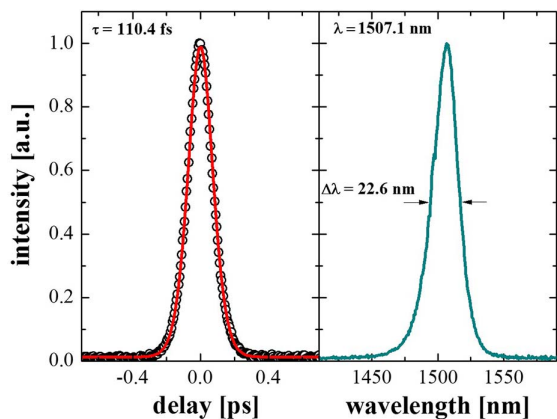


Fig. 4. Autocorrelation trace (left) and the corresponding laser spectrum (right).

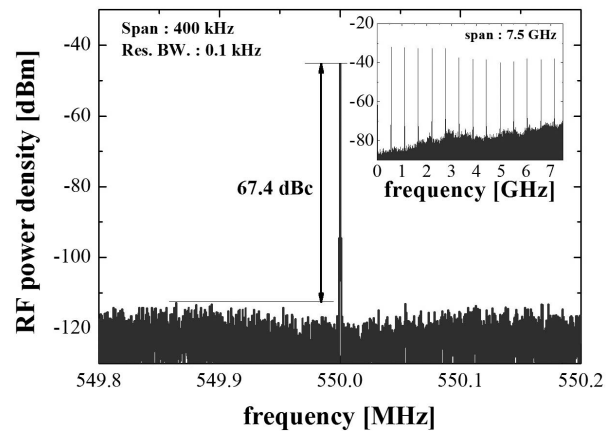


Fig. 5. RF spectra at the fundamental beat note and in a 7.5 GHz span (inset).

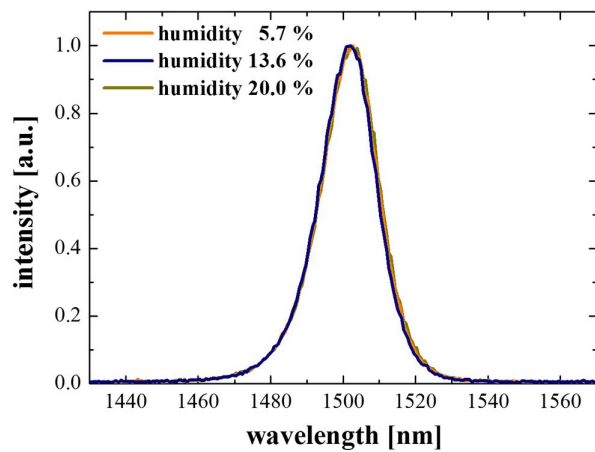


Fig. 6. Mode-locked laser spectra measured at different humidity conditions.

mode-locked operation without any signature of *Q*-switching instabilities or multiple pulsing.

Figure 6 shows the mode-locked spectra for different humidity conditions. To control the humidity, the sealed 500-MHz Cr:YAG laser was purged with nitrogen gas. As shown in Fig. 6, there are no spectral differences for humidity levels of 20.0%, 13.6%, and 5.7%, respectively. Generally, the Cr:YAG laser is quite sensitive to humidity due to the strong water absorption lines around 1.4 μ m. However, in our case, the center wavelength was above 1.5 μ m, so water absorption can be effectively avoided.

In summary, we developed a 550 MHz carbon nanotube mode-locked Cr:YAG laser operating near 1.5 μ m. A CNT-SAM was fabricated for a high-repetition-rate Cr:YAG laser and its nonlinear reflection properties were characterized. By employing the CNT-SAM, we achieved stable and self-starting single-pulse operation of the compact Cr:YAG laser, delivering a maximum output power of 147 mW and a pulse duration of \sim 110 fs at a repetition rate of 550 MHz. To our knowledge, the results present the highest repetition rate among CNT-SAM mode-locked Cr:YAG lasers and the shortest pulse duration among

saturable absorber mode-locked Cr:YAG lasers at a repetition rate of >500 MHz. Considering the low mode-locking thresholds, the CNT mode-locked femtosecond Cr:YAG laser is expected to be used for developing GHz-level bulk laser oscillators near $1.5 \mu\text{m}$. In terms of applications, such $1.5 \mu\text{m}$ coherent sources, which deliver high average output power, short pulse duration, and high repetition rate simultaneously, will improve the signal-to-noise ratio and resolution in nonlinear and time-resolved spectroscopy.

This work was supported by the Korea Electrotechnology Research Institute Primary research program through the National Research Council of Science & Technology (NST) funded by the Ministry of Science, ICT and Future Planning (MSIP) (No. 18-12-N0101-41), the Creative Allied Project of the NST (No. CAP-15-06-ETRI), and the National Research Foundation (NRF) of Korea funded by MSIP (Nos. 2016R1A2A1A05005381 and 2017R1A4A1015426).

References

1. D. Mao, X. Liu, Z. Sun, H. Lu, D. Han, G. Wang, and F. Wang, *Sci. Rep.* **3**, 3223 (2013).
2. A. Bartels, D. Heinecke, and S. A. Diddams, *Science* **326**, 681 (2009).
3. D. A. B. Miller, *IEEE J. Sel. Top. Quantum Electron.* **6**, 1312 (2000).
4. C. Janke, M. Först, M. Nagel, H. Kurz, and A. Bartels, *Opt. Lett.* **30**, 1405 (2005).
5. A. Bartels, T. Dekorsy, and H. Kurz, *Opt. Lett.* **24**, 996 (1999).
6. K. Kieu, W. H. Reminger, A. Chong, and F. W. Wise, *Opt. Lett.* **34**, 593 (2009).
7. S. Y. Choi, D. K. Cho, Y.-W. Song, K. Oh, K. Kim, F. Rotermund, and D.-I. Yeom, *Opt. Express* **20**, 5652 (2012).
8. Y. Ishida and K. Naganuma, *Opt. Lett.* **19**, 2003 (1994).
9. D. J. Ripin, C. Chudoba, J. T. Gopinath, J. G. Fujimoto, E. P. Ippen, U. Morgner, F. X. Kärtner, V. Scheuer, G. Angelow, and T. Tschudi, *Opt. Lett.* **27**, 61 (2002).
10. C. R. Pollock, D. B. Barber, J. L. Mass, and S. Markgraf, *IEEE J. Sel. Top. Quantum Electron.* **1**, 62 (1995).
11. T. Tomaru and H. Petek, *Opt. Lett.* **25**, 584 (2000).
12. T. Tomaru, *Opt. Lett.* **26**, 1439 (2001).
13. C. G. Leburn, A. A. Lagatsky, C. T. A. Brown, and W. Sibbett, *Electron. Lett.* **40**, 805 (2004).
14. B. C. Collings, K. Bergman, and W. H. Knox, *Opt. Lett.* **22**, 1098 (1997).
15. W. B. Cho, J. H. Yim, S. Y. Choi, S. Lee, A. Schmidt, G. Steinmeyer, U. Griebner, V. Petrov, D.-I. Yeom, K. Kim, and F. Rotermund, *Adv. Funct. Mater.* **20**, 1937 (2010).
16. F. Rotermund, W. B. Cho, S. Y. Choi, I. H. Baek, J. H. Yim, S. Lee, A. Schmidt, G. Steinmeyer, U. Griebner, D.-I. Yeom, K. Kim, and V. Petrov, *Quantum Electron.* **42**, 663 (2012).
17. H.-W. Yang, C. Kim, S. Y. Choi, G.-H. Kim, Y. Kobayashi, F. Rotermund, and J. Kim, *Opt. Express* **20**, 29518 (2012).
18. S. Y. Choi, J. W. Kim, M. H. Kim, D.-I. Yeom, B. H. Hong, X. Mateos, M. Aguiló, F. Diaz, V. Petrov, U. Griebner, and F. Rotermund, *Opt. Express* **22**, 15626 (2014).
19. W. B. Cho, A. Schmidt, S. Y. Choi, V. Petrov, U. Griebner, G. Steinmeyer, S. Lee, D.-I. Yeom, and F. Rotermund, *Opt. Lett.* **35**, 2669 (2010).
20. S. D. D. D. Cafiso, E. Ugoletti, A. Schmidt, V. Petrov, U. Griebner, A. Agnesi, W. B. Cho, Y. G. Zhang, S. Y. Choi, F. Rotermund, G. Reali, and F. Pirzio, *Laser Phys. Lett.* **10**, 085801 (2013).
21. C. Hönniger, R. Paschotta, F. Morier-Genoud, M. Moser, and U. Keller, *J. Opt. Soc. Am. B* **16**, 46 (1999).
22. M. Haiml, R. Grange, and U. Keller, *Appl. Phys. B* **79**, 331 (2004).